Remote Sensing of Environment 114 (2010) 1833–1844

Contents lists available at ScienceDirect

Remote Sensing of Environment

journal homepage: www.elsevier.com/locate/rse

# Mapping understory vegetation using phenological characteristics derived from remotely sensed data

Mao-Ning Tuanmu [a,*], Andrés Viña [a], Scott Bearer [b], Weihua Xu [c], Zhiyun Ouyang [c], Hemin Zhang [d], Jianguo Liu [a]

[a] Center for Systems Integration and Sustainability, Department of Fisheries and Wildlife, Michigan State University, East Lansing, MI 48823, USA
[b] The Nature Conservancy, Williamsport Field Office, Williamsport, PA 17701, USA
[c] State Key Laboratory of Regional and Urban Ecology, Research Center for Eco-Environmental Sciences, Chinese Academy of Sciences, Beijing, China
[d] China Conservation and Research Center for the Giant Panda, Wolong Nature Reserve, Wenchuan County, Sichuan Province, China

ARTICLE INFO

*Article history:*
Received 2 October 2009
Received in revised form 16 February 2010
Accepted 17 March 2010

*Keywords:*
Understory vegetation
MODIS
Land surface phenology
Spatial distribution
Habitat modeling

ABSTRACT

Understory vegetation is an important component in forest ecosystems not only because of its contributions to forest structure, function and species composition, but also due to its essential role in supporting wildlife species and ecosystem services. Therefore, understanding the spatio-temporal dynamics of understory vegetation is essential for management and conservation. Nevertheless, detailed information on the distribution of understory vegetation across large spatial extents is usually unavailable, due to the interference of overstory canopy on the remote detection of understory vegetation. While many efforts have been made to overcome this challenge, mapping understory vegetation across large spatial extents is still limited due to a lack of generality of the developed methods and limited availability of required remotely sensed data. In this study, we used understory bamboo in Wolong Nature Reserve, China as a case study to develop and test an effective and practical remote sensing approach for mapping understory vegetation. Using phenology metrics generated from a time series of Moderate Resolution Imaging Spectroradiometer data, we characterized the phenological features of forests with understory bamboo. Using maximum entropy modeling together with these phenology metrics, we successfully mapped the spatial distribution of understory bamboo (kappa: 0.59; AUC: 0.85). In addition, by incorporating elevation information we further mapped the distribution of two individual bamboo species, *Bashania faberi* and *Fargesia robusta* (kappa: 0.68 and 0.70; AUC: 0.91 and 0.92, respectively). Due to its generality, flexibility and extensibility, this approach constitutes an improvement to the remote detection of understory vegetation, making it suitable for mapping different understory species in different geographic settings. Both biodiversity conservation and wildlife habitat management may benefit from the detailed information on understory vegetation across large areas through the applications of this approach.



## 1. Introduction

Understory vegetation plays an important role in forest ecosystems (Gilliam, 2007; Nilsson & Wardle, 2005). Different structure and species compositions of understory plants, including native and exotic species, can affect regeneration of tree species, alter forest succession, and change species diversity through physical, chemical, and biological mechanisms (Royo & Carson, 2006; Urgenson et al., 2009). Understory vegetation also provides essential shelter and food resources for wildlife, and thus its structure and composition is usually associated with the diversity and abundance of many wildlife species (Díaz et al., 2005; Hagar, 2007). Besides its ecological functions in forest ecosystems, non-timber forest products provided by many understory plants (e.g., fibers from bamboo and rattans and medicines from medicinal herbs) are economically important for many countries (Iqbal, 1993). Therefore, understanding the spatio-temporal dynamics of understory vegetation is essential not only for wildlife and biodiversity conservation (Deal, 2007; Estades & Temple, 1999), but also for sustainable forest management (FAO, 1995).

While the importance of understory vegetation is well known, detailed information on its spatial distribution across large areas and its dynamics at fine temporal resolutions is usually unavailable because conventional methods for gathering vegetation information emphasize on ground-based surveys, which are time-consuming, labor-intensive, and sometimes logistically unfeasible. Although remote sensing is a useful alternative tool for gathering vegetation information across large areas and over time (Jensen, 2007; Roughgarden et al., 1991), remote detection of understory plants is limited due to the interference of overstory canopies. While the presence of understory vegetation influences the

* Corresponding author. Center for Systems Integration and Sustainability, 1405 S. Harrison Road, Suite 115 Manly Miles Bldg., Michigan State University, East Lansing, MI 48823-5243, USA. Tel.: +1 517 432 5074; fax: +1 517 432 5066.
*E-mail address:* tuanmuma@msu.edu (M.-N. Tuanmu).

0034-4257/$ – see front matter © 2010 Elsevier Inc. All rights reserved.
doi:10.1016/j.rse.2010.03.008

signals received by remote sensors, its relative contributions to the signals vary with the structure and species composition of both over and understory vegetation (Eriksson et al., 2006; Rautiainen et al., 2007). Because of the complex and non-linear interactions between the reflectance of over and understory components, distinguishing the signals of understory vegetation from overstory canopies and characterizing understory vegetation are challenging.

Many efforts have been made to overcome this challenge via advanced classification algorithms. For instance, using artificial neural networks to capture the non-linear relationship between the reflectance of over and understory vegetation, Linderman et al. (2004) have successfully detected understory bamboo distribution with an overall accuracy of 80% (and a kappa statistic of 0.56, which we calculated from the confusion matrix reported in Table 3 of Linderman et al., 2004). Wang et al. (2009a) classified an Advanced Spaceborne Thermal Emission and Reflection Radiometer (ASTER) image into three understory cover classes with a kappa statistic of 0.60 by integrating a neural network and a Geographic Information System (GIS) expert system. However, applying these methods in a larger spatial extent may be limited by the availability of cloud-free images with high spatial resolutions, and locally specific rules in the expert system.

Other studies have used active sensor systems. For example, data acquired using Light Detection and Range (LiDAR) sensors have been used to characterize the three-dimensional structure of forests (Lefsky et al., 2002; Vierling et al., 2008), and map understory plants in boreal forests (Korpela, 2008; Peckham et al., 2009). Combined with hyperspectral images, LiDAR data have also been used to map an understory invasive species in tropical forests (Asner et al., 2008). However, the most important limitation for ecological applications of these airborne sensor data is their high acquisition costs and low availability, especially in developing countries (Vierling et al., 2008).

Differences in phenology between over and understory vegetation have also been used to detect understory vegetation. For instance, due to the earlier senescence of tree leaves as compared to the leaves of an understory invasive shrub species, Resasco et al. (2007) found that stands with high coverage of the understory shrub could be separated from those with low/zero coverage using late-fall Landsat imagery. In addition, Chastain and Townsend (2007) and Wang et al. (2009b) also successfully used leaf-off Landsat images to detect evergreen understory vegetation under deciduous forests (with kappa statistics of 0.755–0.806 and 0.59, respectively). However, the limited temporal windows when the phenological difference between over and understory can be detected further reduce the data availability. Furthermore, the inter-annual variability of vegetation phenology due to variable climatic conditions may change the optimal dates for separating over and understory components in different years (Resasco et al., 2007).

High temporal resolution remotely sensed data, such as those collected by the Moderate Resolution Imaging Spectroradiometer (MODIS), may provide a solution for the problem of mapping understory vegetation across large areas. With high frequency of acquisitions, those data reduce the problem of cloud contamination and provide detailed information on the temporal dynamics of the land surface. As vegetation phenology causes changes in surface reflectance over time, they can be captured by multi-temporal remotely sensed data (Ahl et al., 2006; Reed et al., 1994; Schwartz & Reed, 1999). The phenological patterns captured by remotely sensed data are termed land surface phenology (Friedl et al., 2006), in order to distinguish them from the traditional definition of vegetation phenology. Previous studies have shown that these phenological characteristics are useful for classifying different land cover types (DeFries et al., 1995; Hansen et al., 2000; Lloyd, 1990), monitoring land cover change (de Beurs & Henebry, 2004; Lenney et al., 1996), and differentiating forest classes and types (Townsend & Walsh, 2001). However, the phenological characteristics captured by multi-temporal remotely sensed data are affected by not only the dominant overstory vegetation, but also the understory vegetation. Viña et al. (2008) have shown that the seasonal patterns of vegetation indices derived from MODIS data were different between forests with similar overstory vegetation but with different understory coverage. This conspicuous difference in phenological patterns suggests that land surface phenology has the potential to be used for mapping understory vegetation across large areas.

The main goal of this study was to develop an approach for deriving detailed information on the spatial distribution of understory vegetation using the phenological patterns detected by multi-temporal remotely sensed data. We selected the bamboo species living under the canopy of temperate forests in Wolong Nature Reserve, China as a case study. Because bamboo species dominate the understory vegetation within this region and provide essential food for several wildlife species (Schaller et al., 1985) including the endangered giant panda (*Ailuropoda melanoleuca*), identifying their spatial distribution has direct wildlife conservation implications. To develop and test our approach, we (1) generated phenology metrics from a time series of MODIS data and examined the phenological characteristics of forests with understory bamboo; (2) generated a spatial model for mapping understory bamboo distribution using field data, phenology metrics, and species distribution modeling; and (3) explored the potential application of this approach to mapping and differentiating individual bamboo species.

## 2. Methods

### 2.1. Study area

Wolong Nature Reserve, China (Fig. 1), which lies between the Sichuan basin and the Tibetan highlands, is characterized by a wide vertical variation in topography, climate and soils, together with a diverse flora and fauna. As one of the largest nature reserves (ca. 2000 $km^2$) established for giant panda conservation, it includes around 10% of the entire wild panda population (State Forestry Administration, 2006). It also contains around 4000 plant species, 102 mammal species and more than 230 breeding bird species (Wolong Nature Reserve and Sichuan Normal College, 1992). Natural vegetation in the reserve varies along the elevation gradient (Schaller et al., 1985). Broadleaf forests are dominated by evergreen species below 1600 m, and by a mixture of evergreen and deciduous species between 1600 and 2000 m. Above 2000 m, a mixed coniferous and deciduous broadleaf forest gradually changes to a subalpine coniferous forest around 2600 m. The forest reaches about 3600 m until it is replaced by alpine meadows. Under forest canopies, evergreen bamboo species dominate the understory layer. Seven native bamboo species are found in the reserve, but two of them, arrow bamboo (*Bashania faberi*) and umbrella bamboo (*Fargesia robusta*), are dominant and constitute the major food for giant pandas (Schaller et al., 1985). While arrow bamboo is mainly distributed between 2500 and 3400 m in elevation, umbrella bamboo usually occurs between 1600 and 2650 m.

### 2.2. Field data

We obtained bamboo presence data from the Third National Giant Panda Survey (State Forestry Administration, 2006). Survey teams collected field data following transects across different vegetation types during the summer of 2001. Along the transects, surveyors recorded, using Global Positioning System receivers, the geographic locations of 468 sites with signs of giant panda activity, including fecal droppings, feeding sites, dens, footprints, and visual sightings. In each site, surveyors identified bamboo species and assigned the coverage of understory bamboo to one of four categories (0–24%, 25–49%, 50–74% and 75–100%). Because low bamboo cover has a limited contribution to the surface reflectance registered by satellite sensors and may not provide enough food or shelter for wildlife species, we only used the locations where bamboo cover was estimated to be 25% or higher (Fig. 1). In these locations, besides the two dominant bamboo species, *F. nitida* and *Yushania brevipaniculata* were also found. Although

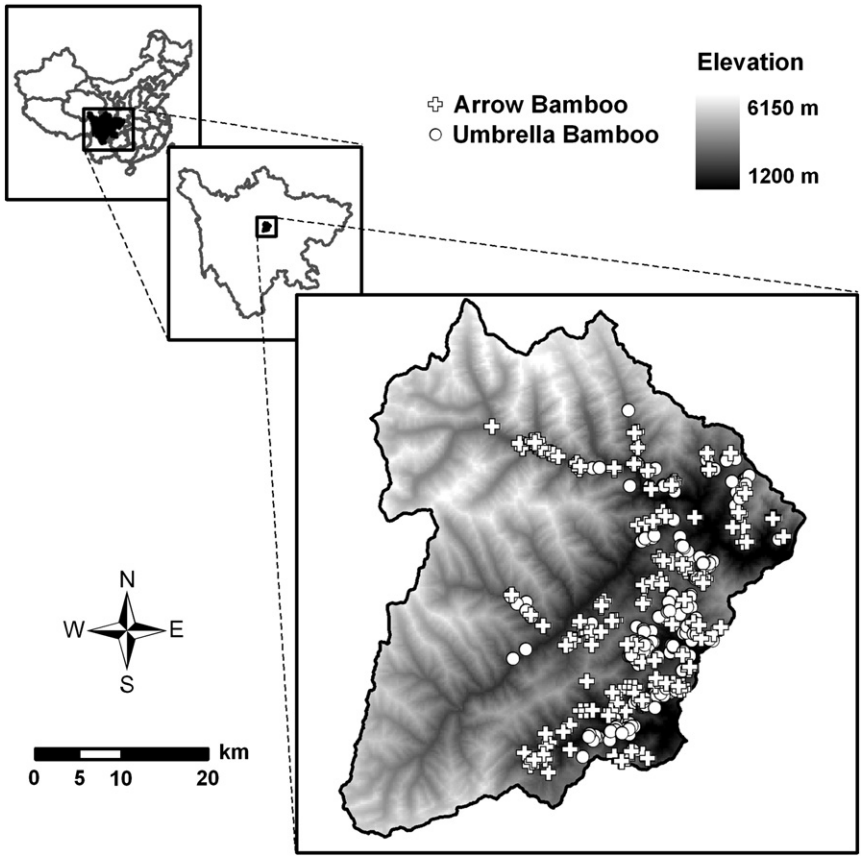


**Fig. 1.** Location and topography of Wolong Nature Reserve in Sichuan Province, China. Also shown are the locations of the field plots where arrow or umbrella bamboo cover was 25% or higher according to the Third National Giant Panda Survey conducted in 2001.

bamboo species may occur in shrubland, in the study area shrubland with bamboo is only found in small patches within clear-cut areas for past timber production (Reid et al., 1991; Schaller et al., 1985). In addition, only one of the 468 field sites has a vegetation type of shrubland with bamboo species in the dataset. Therefore, we excluded that site from the following analyses and focused on the bamboo under forests in this study.

### 2.3. Remotely sensed data and phenology metrics

We obtained a time series of MODIS surface reflectance imagery (8-day L3 Global 250 m product, MOD09Q1) acquired between May 2000 and April 2004 through the Land Processes Distributed Active Archive Center (https://lpdaac.usgs.gov/). Using the surface reflectance values in the red ($R_{RED}$, 620–670 nm) and near infrared ($R_{NIR}$, 841–876 nm) spectral bands, we calculated the Wide Dynamic Range Vegetation Index (WDRVI) (Gitelson, 2004):

$$WDRVI = (\alpha \cdot R_{NIR} - R_{RED}) / (\alpha \cdot R_{NIR} + R_{RED}) \quad (1)$$

where $\alpha$ is a weighting coefficient set as 0.25 following Henebry et al. (2004). This coefficient reduces the saturation problem of the Normalized Difference Vegetation Index (NDVI) under moderate-to-high biomass conditions (Gitelson, 2004). The WDRVI has been proved to be linearly related with leaf area index (LAI) and sensitive to changes in LAI up to 6 (Gitelson, 2004; Viña et al., 2004b). Therefore, the WDRVI appears to be more suitable than the widely-used NDVI for studying the changes in green biomass under high LAI values, such as the forests with dense understory bamboo in our study area. In order to further reduce the cloud contamination, which lowered WDRVI values, we generated a time series of 16-day composites using the maximum value between two consecutive 8-day periods.

Using TIMESAT 2.3 (Jönsson & Eklundh, 2004, 2006), we smoothed the time series (May 2000–April 2004) of 16-day WDRVI composites for each pixel by means of the adaptive Savitzky–Golay filter. With these data we obtained three full phenological cycles (2001–2003) and calculated 11 phenology metrics for each cycle: (1) the base level, corresponding to the average between the starting and ending minimum values of each cycle (A in Fig. 2); (2) the maximum level, corresponding to the highest value in each cycle (B in Fig. 2); (3) the amplitude, calculated as the difference between the maximum and the base levels (C in Fig. 2); (4) the date of the start of the season (*SOS*), determined as the date when WDRVI values increase to 20% of the difference between the maximum WDRVI value and the minimum value at the start of each cycle (D in Fig. 2); (5) the date of the end of the season (*EOS*), defined as the date when WDRVI values decrease to 20% of the difference between the maximum value and the minimum value at the end of each cycle (F in Fig. 2); (6) the date of the middle of the season (*MOS*), determined as the median of the two dates when WDRVI values increase (decrease) to 80% from the minimum value at the start (end) of each cycle (E in Fig. 2); (7) the length of the season, defined as the difference between *SOS* and *EOS* (G in Fig. 2); (8) the large integral, obtained as the area under the smoothed curve between *SOS* and *EOS* (H in Fig. 2); (9) the small integral, defined as the large integral minus the area below the base level (I in Fig. 2); (10) the increase and (11) decrease rates, calculated as the slopes of two lines across the 20% and 80% level points on the left and right sides of the MOS, respectively (J and K in Fig. 2).

In some pixels, phenology metrics could not be obtained on a particular cycle due to either lack of detectable phenological cycles or incomplete cycles within a year. To reduce both the effects of missing

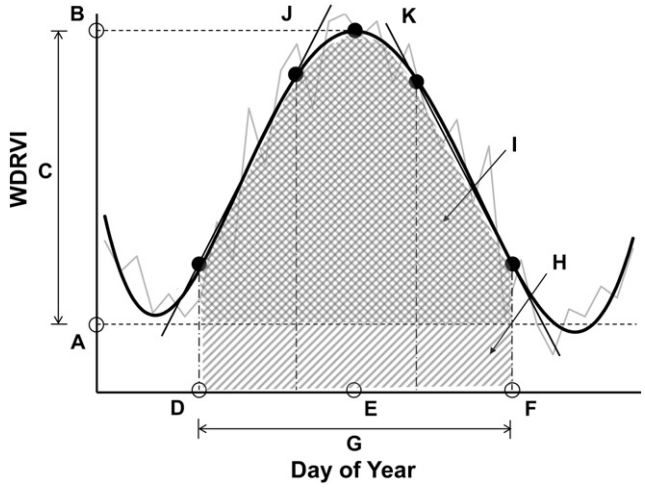


**Fig. 2.** Phenology metrics determined from a smoothed curve of a time series of WDRVI values. A — base level; B — maximum level; C — amplitude; D — date of the start of the season; E — date of the middle of the season; F — date of the end of the season; G — length of the season; H — large integral; I — small integral; J — increase rate; and K — decrease rate.

cycles and inter-annual variability in phenology metrics, we calculated the average of the annual values from 2001 to 2003 for each pixel. We treated the pixels which had less than two valid annual values as missing data and excluded them from the following analyses.

### 2.4. Phenological characteristics of forests with understory bamboo

To test whether the phenological characteristics of the forests with understory bamboo can be distinguished from other land cover types using the 11 phenology metrics, we compared them among five groups of pixels. For the first group (*All*), we randomly selected 1000 pixels from the study area as a representative of the entire area. The second group (*For*) was a random selection of 1000 pixels with a forest cover. Pixels with a forest cover were determined based on a binary forest cover map derived from a Landsat-5 Thematic Mapper image acquired on 13 June 2001 (Viña et al., 2007) and resampled to 250×250 m/pixel using the majority algorithm. A series of tests on the selected pixels' representativeness of the entire study area and forest area indicated that the variation of the means of pixel values (i.e., values of each phenology metric) decreased with the increase in the number of selected pixels, but the change became negligible when more than 500 pixels were selected (results not shown). On the other hand, selecting more pixels may increase the spatial autocorrelation among selected pixels. To achieve representativeness and reduce the effects of spatial autocorrelation on statistical tests (see below), we used 1000 randomly selected pixels in this analysis. The third group (*Bam*) contained 356 pixels where bamboo cover was 25% or higher (including all four bamboo species, i.e., *B. faberi*, *F. robusta*, *F. nitida* and *Y. brevipaniculata*) according to the field data. The remaining two groups were composed of 145 pixels where arrow bamboo cover was 25% or higher (*Arr*), and 184 pixels where umbrella bamboo cover was 25% or higher (*Umb*), respectively. We then compared the pixel values between each pair of the five groups using the Mann–Whitney *U*-test for each of the 11 phenology metrics. We used this non-parametric test because the pixel values were not normally distributed, according to a Shapiro–Wilk normality test performed (results not shown). The conclusions on significant differences drawn from this test are more conservative since the non-parametric *U*-test is less powerful to detect significant differences between groups, as compared to parametric methods (e.g., *t*-test) (Sheskin, 2000).

For this analysis, we conducted presence vs. background comparisons (e.g., forest pixels with bamboo vs. random selection of all forest pixels), rather than presence vs. absence comparisons (e.g., forest pixels with bamboo vs. forest pixels without bamboo) mainly for two reasons. First, although possible, it is not practical to confirm absolute absence of understory species across a 6.25 ha field plot (i.e., the spatial resolution of a 250×250 m MODIS pixel). Second, the modeling algorithm used to map understory bamboo is based on the difference in the values of predictor variables obtained in presence locations and in background (i.e., random) locations (see Section 2.5). Therefore, the presence vs. background comparisons examined the information content of the data directly used by the modeling algorithm to map understory vegetation.

### 2.5. Overall bamboo distribution

In order to distinguish the pixels with understory bamboo from the others based on their phenological characteristics, we used the maximum entropy modeling framework (Maxent). Maxent is an algorithm designed to make predictions based on incomplete information (Phillips et al., 2006) and has been proven to be one of the best methods for mapping species distribution (Elith et al., 2006). The algorithm contrasts the environmental conditions (characterized in a multi-dimensional space defined by environmental variables) in species presence locations vs. the conditions in background locations (i.e., the entire study area). It then establishes the species–environment relationship by matching the contrasts and approaching a maximum entropy distribution (i.e., maximum uniform distribution) simultaneously (Phillips et al., 2006). The relationship can be used to estimate the probability of species occurrence across the entire study area given the spatial patterns of the environmental variables (Phillips et al., 2006; Phillips & Dudík, 2008).

Besides its good performance on mapping species distribution (Elith et al., 2006), Maxent also has several characteristics which make it suitable for mapping understory vegetation based on phenological characteristics obtained from MODIS data. First, it uses presence-only, rather than presence/absence data. This is important since it is not logistically feasible to confirm absence of understory bamboo in an entire 250×250 m area. Using the presence-only procedure, we can avoid the potential biases caused by uncertain or false absence data. In addition, like other machine learning methods (e.g., neural networks), Maxent can capture complex and non-linear species–environment relationships, even with noise in input data (Elith et al., 2006; Phillips et al., 2006). Finally its continuous output values, i.e., species presence probabilities, make Maxent a fuzzy classifier that provides more detailed information on understory vegetation distribution than binary outputs (i.e., presence/absence).

We used the software Maxent (version 3.3.1, http://www.cs.princeton.edu/~schapire/maxent/, Phillips et al., 2006) to generate a model for mapping overall bamboo distribution. For generating the model, we used the pixels whose bamboo cover was 25% or higher (including all four bamboo species) as presence data, 10,000 pixels randomly selected from the study area as background data following the suggestions of Phillips and Dudík (2008), and the 11 phenology metrics derived from a time series of MODIS-WDRVI values as predictor variables. We used 70% of the bamboo presence data (249 pixels) as a training dataset and the remaining 30% (107 pixels) as a validation dataset. In order to reduce the potential effects of the random data partitioning, we ran the model 20 times (replicates) with different random data partitions for each run and averaged the predicted bamboo presence probabilities over the 20 runs for each pixel. This number of replicates was used because pilot tests showed the variation of model outputs, measured as the mean of standard deviations among different runs, decreased with the increase in the number of runs, but changed negligibly after 20 runs.

### 2.6. Individual bamboo distribution

Besides mapping overall bamboo distribution, we also explored the ability of our approach to map individual bamboo species. With

the same method described earlier, we generated a model and obtained the average of presence probabilities over 20 model runs for each of the two dominant bamboo species, i.e., arrow and umbrella bamboo. Because the two bamboo species are distributed within different elevation ranges, we hypothesized that adding elevation information into the model would improve the model's ability to separate the two species. To test this hypothesis, besides the model generated with 11 phenology metrics, we also generated a model using elevation as an additional predictor variable and compared the model performance (see Section 2.7) between the two models. We obtained the information on elevation from a digital elevation model created by the Shuttle Radar Topography Mission and resampled the original data to 250×250 m/pixel using the nearest neighbor algorithm to keep consistent spatial resolution with the other data.

### 2.7. Model validation and comparison

We used both threshold-dependent and threshold-independent methods to validate models and evaluate their performance. The Cohen's kappa analysis, a chance-corrected measure of agreement (Cohen, 1960), was selected for the threshold-dependent method because it is commonly used for evaluating classification accuracy of remote sensing imagery and also used in previous studies on mapping understory vegetation (Chastain & Townsend, 2007; Wang et al., 2009a,b). The kappa value ranges between 0 and 1 with a larger value indicating better model performance (Cohen, 1960). Model performance can be judged as excellent if kappa>0.75, good if 0.75>kappa>0.4, or poor if kappa<0.4 (Araújo et al., 2005; Landis & Koch, 1977). Because only presence data on bamboo distribution were available, we performed the analysis by contrasting presence pixels to those randomly selected from the study area (background pixels). To avoid the potential failure of kappa analysis with unbalanced validation data (McPherson et al., 2004), we randomly selected 100 background pixels to make the number be close to the number of presence pixels in validation datasets (i.e., 30% of bamboo presence data or 107 pixels). The threshold for cutting off continuous outputs from each model run was determined by the kappa maximization approach, which finds the threshold corresponding to the maximum kappa value (Liu et al., 2005). Because 100 pixels (ca. 0.3% of total pixels) were not representative of the entire area, we calculated 30 kappa values for each model run by using the same presence pixels but different 100 random background pixels, and then obtained an average of the 30 values.

The receiver operating characteristic (ROC) analysis, a threshold-independent method, is also a widely-used method for evaluating the accuracy of classification models (Fielding & Bell, 1997; Pearce & Ferrier, 2000). The ROC curve is generated by plotting sensitivity values (i.e., fraction of true positive) against 1-specificity values (i.e., fraction of false positive) for every possible threshold (Hanley & Mcneil, 1982). The area under the ROC curve (AUC) provides a single-value measurement of model performance. Since omission errors reduce sensitivity and commission errors reduce specificity, both types of errors equally reduce the AUC value. While an AUC value of 1 indicates a perfect model, a value of 0.5 indicates a random model. A standard for judging model performance based on AUC values (Araújo et al., 2005; Swets, 1988) is: excellent (AUC>0.9), good (0.9>AUC>0.8), fair (0.8>AUC>0.7), poor (0.7>AUC>0.6), and failed (0.6>AUC>0.5). Similar to the calculation of the kappa statistic, we also used presence/background validation data for calculating AUC values. However, because AUC values are not sensitive to unbalanced validation data (McPherson et al., 2004; Zweig & Campbell, 1993) and no statistical test is involved in the calculation of AUC values, the number of background pixels does not affect the calculated values if the background pixels are representative of the entire study area. Therefore, we used the default background pixels in the Maxent software (i.e., 10,000 background pixels) to calculate AUC values.

By using presence/background data, the kappa and AUC values calculated in this study tend to be underestimated because some of the background pixels are actually presence pixels, which artificially increase commission errors. In addition, the degree of underestimation is determined by the proportion of actual presence pixels in the background pixels, which is, in turn, determined by the actual proportion of habitat in the entire study area. Since the actual proportion of habitat is almost always unknown, direct comparisons of the values calculated in this study with the values reported in other studies should be done with caution. Comparisons between different models using these statistics are valid only if the models are generated for the same species in the same study area and are evaluated using the same presence/background data, as was done in this study (see below).

In order to examine the relative importance of each phenology metric for mapping bamboo distribution, we conducted a jackknife analysis on model performance by using the Maxent software. For this, the software calculated the AUC values of models containing only one of the 11 metrics and of models containing all, but one of the metrics used as predictor variables, through a jackknife resampling approach. In this analysis, a higher AUC value for a model containing only one metric indicates that the specific metric is more informative for mapping bamboo distribution than other metrics. In contrast, a lower AUC value for a model without one specific metric indicates that the metric contains more information for mapping bamboo not provided by the other metrics.

For comparing the performance of the individual bamboo models with and without elevation information, besides calculating kappa and AUC values, we also used the minimum predicted area (MPA) method (Engler et al., 2004). The MPA is the minimum area which is constituted by all pixels whose species presence probabilities are above a defined threshold and encompasses a specified percentage (e.g. 95%) of presence locations (Engler et al., 2004). With presence-only validation data, a model predicting species present everywhere has the best performance because it correctly predicts all presence locations, but the model is useless. Therefore, the MPA method evaluates model performance based on the parsimonious concept that a good model should predict the habitat as small as possible (i.e., with low commission errors), but it still encompasses a maximum number of presence locations (i.e., with low omission errors). In this analysis, a threshold was selected for each model run so that the pixels with probabilities above the threshold encompassed 95% of presence locations. Kappa and AUC values and the proportions of MPA to the whole study area obtained for 20 runs of the models with and without elevation were compared using Mann–Whitney *U*-tests.

## 3. Results

### 3.1. Phenological characteristics of forests with understory bamboo

Because of a lack of detectable seasonal cycles or incomplete annual cycles in at least two years, phenology metrics could not be calculated in 289 pixels (i.e., 0.76% of the total number of pixels) of the entire study area. Among these pixels, only 112 pixels (i.e., 0.79% of the total number of forest pixels) were covered by forests, according to the forest cover map, and none of them contained field plots with 25% or higher bamboo cover. Therefore, the impact of their exclusion from the analysis is negligible due to the small proportions of these pixels in the five pixel groups.

Significant differences in the values of 11 phenology metrics were found among the five groups of pixels (Fig. 3), even with the more conservative significant tests conducted using the non-parametric method. Compared to the pixels randomly selected from the whole study area (*All*), the pixels with understory bamboo (*Bam*) had significantly ($p<0.001$) higher base and maximum levels, a higher amplitude, earlier SOS and MOS, a longer length of season, and higher large and small integrals (Fig. 3). Compared to pixels with forest cover (*For*), the pixels of the *Bam* group had a significantly higher maximum level, a higher amplitude, earlier SOS, MOS, and EOS, higher large and small

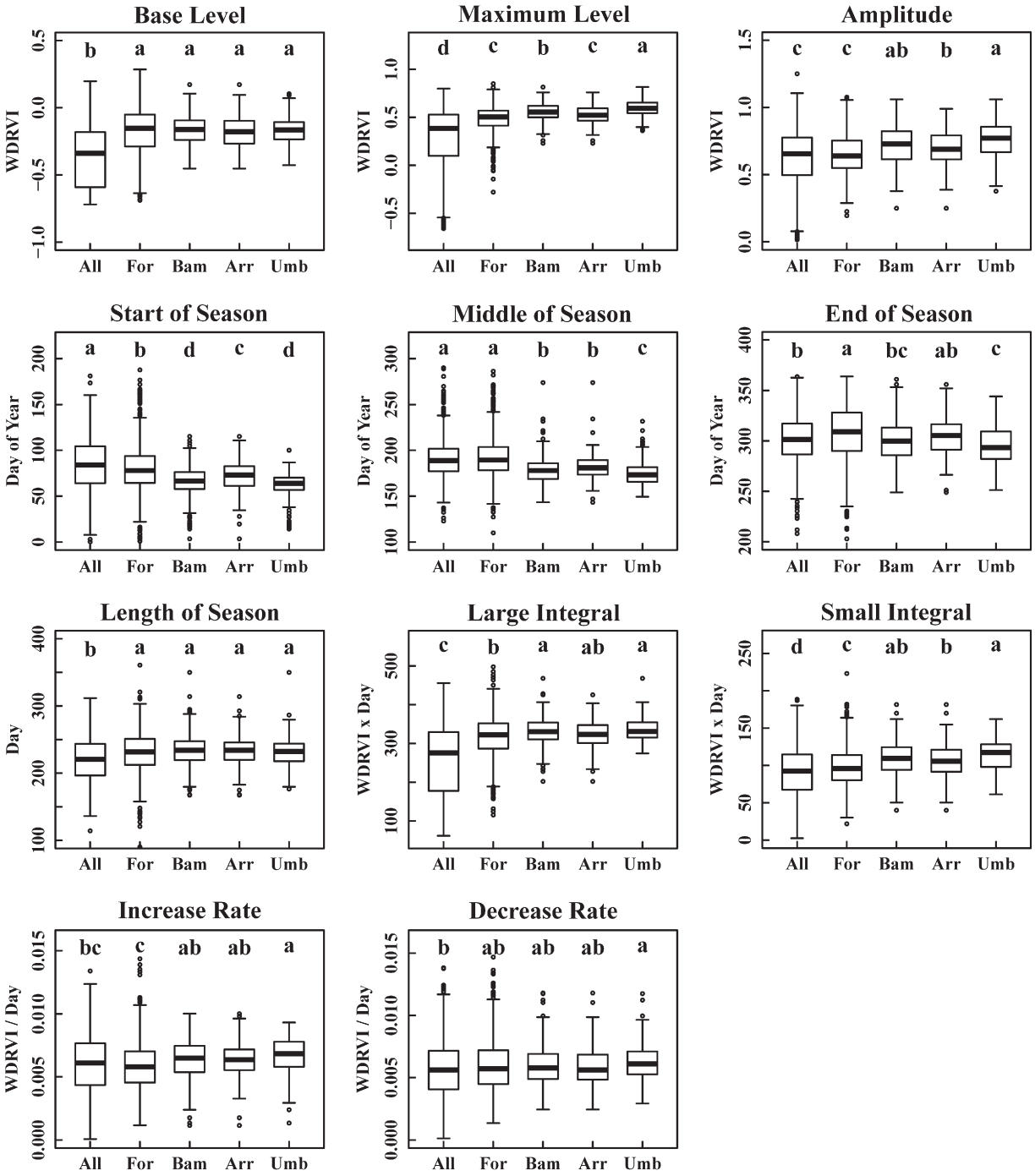


**Fig. 3.** Box plots of 11 phenology metrics calculated using 1000 pixels randomly selected from the entire study area (*All*), 1000 pixels randomly selected from forested areas (*For*), 356 pixels where field plots with bamboo cover as 25% or higher were located (*Bam*), 145 pixels where field plots with arrow bamboo cover as 25% or higher were located (*Arr*), and 184 pixels where field plots with umbrella bamboo cover as 25% or higher were located (*Umb*). The dark line inside a box indicates the median; the bottom and the top of a box show the 25th and 75th percentiles, respectively; the ends of the two whiskers indicate the lowest and the highest values within 1.5 interquartile ranges from a box; dots beyond whiskers show outliers whose values were outside the range indicated by the whiskers. The letters above boxes show the results of pair-wise comparisons on the phenology metric values conducted using Mann–Whitney *U*-tests. Two boxes share the same letter if there was no significant difference ($p>0.001$) between them.

integrals, and a higher increase rate (Fig. 3). While the values of the pixels with arrow bamboo (*Arr*) were significantly different in eight and five of the 11 metrics from the *All* and *For* groups, respectively, they were different from the *Bam* group only in the maximum level and SOS (Fig. 3). The values of pixels with umbrella bamboo (*Umb*) were significantly different from the *All* and *For* groups in all and eight of the metrics, respectively (Fig. 3). However, significant differences were found only in the maximum level and MOS between the *Umb* and *Bam* pixels (Fig. 3).

### 3.2. Overall bamboo distribution

The kappa and AUC values (mean ± 2 SEM) of the 20 runs of the overall bamboo distribution model were 0.591 ± 0.018 and 0.851 ± 0.005, respectively. Both values, even though underestimated due to the use of presence/background validation data, indicated a good model according to the judgment standards (Araújo et al., 2005; Landis & Koch, 1977; Swets, 1988). The estimated bamboo presence probabilities for pixels ranged between 0 and 0.9 across the study area, with higher

probability values occurring at low- and mid-elevations (Fig. 4a). The highest standard deviation of the estimated presence probabilities was 0.3, but most pixels had standard deviations lower than 0.05 (Fig. 4b). The low standard deviations indicated that the estimated probabilities did not change much with different data partitioning for training and validation datasets. Among the pixels whose phenology metrics could not be calculated, 137 were located above 3600 m, thus beyond the distribution range of forests and bamboo species in the study area, and 40 of the other pixels were not covered by forests, according to the forest cover map. Therefore, the missing data may affect the estimated bamboo presence probabilities in only 112 pixels (i.e., 0.29% of the total number of pixels).

The results of the jackknife analysis on the relative importance of phenology metrics for mapping understory bamboo are shown in Fig. 5. The models with only the maximum level, base level, or large integral had the highest AUC values (Fig. 5a), which indicated that those metrics contained the most useful information for mapping understory bamboo. The models without the SOS, small integral, or base level had the lowest AUC values (i.e., largest loss in AUC) (Fig. 5b), and thus those metrics contained unique information for mapping bamboo distribution.

### 3.3. Individual bamboo distribution

Although the mean kappa and AUC values indicated that the performance of the arrow and umbrella bamboo models without elevation was fair to good and good to excellent, respectively (Table 1), the models could not effectively differentiate the distribution of the two species. While umbrella bamboo had higher presence probabilities at relatively lower elevations (Fig. 6b), consistent with the field data and our knowledge about the general distribution pattern of this species, the estimated probabilities for arrow bamboo were also high in some low-elevation areas (Fig. 6a). The relatively low kappa and AUC values obtained for arrow bamboo (Table 1) seem to reflect this overestimation at lower elevations.

With the incorporation of elevation information, the mean kappa and AUC values increased and the proportion of MPA decreased significantly for both species (Table 1). Higher kappa and AUC values and smaller MPA suggested that model performance on mapping individual bamboo species was significantly improved with the addition of elevation as a predictor variable. In addition, the spatial patterns of estimated presence probabilities also showed that the distribution patterns of the two bamboo species can be differentiated (Fig. 6c and d) with the incorporation of elevation information into the models.

## 4. Discussion

In this study, we developed an effective approach for mapping understory vegetation across large spatial extents using remotely sensed data. By taking the advantage of MODIS data's high temporal resolution, we captured the phenological characteristics, in terms of WDRVI values, of forests with understory bamboo using phenology metrics. We then established the relationship between bamboo presence and phenological characteristics and used it to map understory bamboo by using Maxent. With this approach, we successfully mapped the spatial distribution of bamboo species under temperate forests in Wolong Nature Reserve, China. While land surface phenology derived from time series of remotely sensed data has been used for land cover classification (DeFries et al., 1995), vegetation change detection (de Beurs & Henebry, 2004; de Beurs & Henebry, 2005), canopy phenology monitoring (Ahl et al., 2006; Viña et al., 2004a; Zhang et al., 2003), invasive plant mapping and monitoring (Huang et al., 2009; Morisette et al., 2006), and wildlife habitat characterization (Viña et al., 2008), in this study its applications have been extended to evaluate the spatial distribution of understory plant species growing under a forest canopy.

By analyzing the land surface phenology characterized by phenology metrics, we found that forest pixels with understory bamboo can be distinguished from background and forest pixels in the whole study area. While higher base and maximum levels, an earlier SOS, a longer season length, and higher large and small integrals reflected the difference between forests and other land cover types (Fig. 3), a still higher maximum level, much earlier SOS and MOS, higher yet integrals, and a higher increase rate showed the contributions of bamboo species to the land surface phenology of forest pixels with understory bamboo (Fig. 3). The high biomass and annual net primary productivity of understory bamboo (dry weights: 5–12 ton $ha^{-1}$ and 1.2–1.9 ton $ha^{-1}$ $year^{-1}$ for arrow bamboo and 15–40 ton $ha^{-1}$ and 1.5–3.9 ton $ha^{-1}$ $year^{-1}$ for umbrella bamboo) in the study area (Taylor & Qin, 1993) may account for the higher maximum level and integrals. The rapid growth in the height of bamboo shoots during the early growing season (Qin et al., 1993; Taylor & Qin, 1993) may be the reason for the higher increase rate and earlier SOS of the pixels with bamboo.

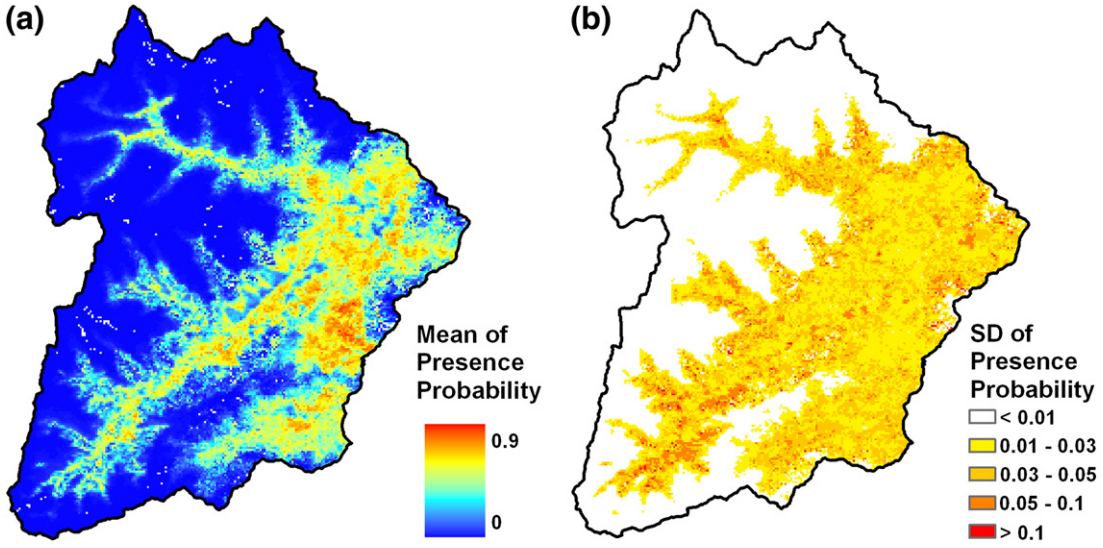


**Fig. 4.** Overall bamboo distribution across Wolong Nature Reserve. The pixel-wise (a) mean values and (b) standard deviations of bamboo presence probabilities were calculated over 20 runs of the overall bamboo distribution model. The model was generated using 356 pixels with 25% or higher bamboo cover as presence locations and 11 phenology metrics as predictor variables. The 289 pixels where phenology metrics could not be determined in at least two years between 2001 and 2003 from a smoothed curve of a time series of WDRVI values by TIMESAT are represented in white.

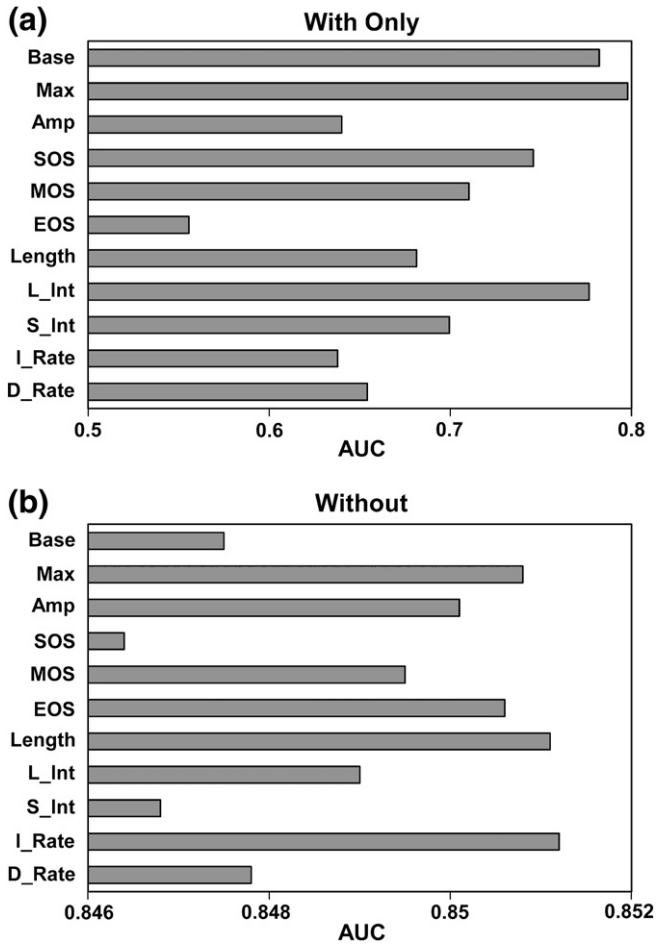


**Fig. 5.** Mean AUC values of the overall bamboo distribution models (a) with only one of the 11 phenology metrics and (b) with all, but one, metrics as predictor variables. A higher AUC value for a model with only one metric indicates that the metric contained more useful information for mapping bamboo distribution in the full model. A lower AUC value (larger loss of the AUC value) for a model without one metric indicates that the metric contained more information which cannot be represented by the other metrics for mapping bamboo distribution. Max — maximum level; Amp — amplitude; SOS — date of the start of the season; MOS — date of the middle of the season; EOS — date of the end of the season; L_Int — large integral; S_Int — small integral; I_Rate — increase rate; and D_Rate — decrease rate.

Since the bamboo species in the study area are evergreen, it was expected that their contribution to the green biomass was larger when overstory tree leaves undergo senescence (e.g., during winter months). However, no difference in the base level between forests with bamboo and background forests was observed. This result could be partially explained by snow cover during the winter months. Although bamboo species under evergreen coniferous forests may not cause difference in land surface phenology as much as those under deciduous or mixed forests, pure evergreen coniferous forests are rare in the study area. While firs (e.g., *Abies faxoniana*) are dominant in the subalpine coniferous forests above 2600 m in elevation, birches (e.g., *Betula utilis* and *B. albosinensis*) and rhododendrons (e.g., *Rhododendron oreodoxa* and *R. watsonii*) are also abundant (Schaller et al., 1985). However, although it is not a major concern in this study, the potential effect of evergreen overstory on the detectability of phenological difference caused by understory vegetation needs further study. In addition, besides the direct contribution of understory bamboo, the difference in canopy tree species composition and density caused by different understory bamboo cover (Taylor et al., 2004, 2006) may also affect the land surface phenology. Therefore, further studies on the phenology of canopy trees and understory bamboo measured on the ground are needed for understanding the phenological characteristics captured by remotely sensed data.

According to the jackknife analysis, the most important predictor variables containing either the most useful or the most unique information for mapping understory bamboo were the base and maximum levels, SOS, and large and small integrals (Fig. 5). Significant differences between forest pixels with bamboo versus background pixels of the whole study area were observed in all of these five metrics (Fig. 3). In addition, except for the base level, the other four metrics were also significantly different between forests with bamboo versus background forests (Fig. 3). The results of these two analyses and the consistence between them indicate that the good performance of the approach developed in this study on mapping understory bamboo is due to (1) the ability of phenology metrics derived from a time series of MODIS data to capture differences in land surface phenology caused by understory bamboo, and (2) the ability of Maxent to extract and use the phenological difference for mapping bamboo distribution.

Besides the good agreement between the field data and the bamboo distribution maps generated in this study, our approach has several improvements on mapping understory vegetation as compared to other methods. First, our approach is more suitable for mapping the spatial patterns and monitoring temporal dynamics of understory vegetation across large areas. While several previous approaches have been proved useful for detecting understory vegetation at local scales (Korpela, 2008; Linderman et al., 2004; Resasco et al., 2007; Wang et al., 2009a,b), their applications to broader scales may be limited due to cloud contamination (e.g., Landsat data), high acquisition costs (e.g., LiDAR data) and/or lack of images acquired during specific time periods (e.g., leaf-off seasons). In contrast, our approach solves the problem of data availability by using MODIS data, which have been acquired daily and globally since 24 Feb. 2000 and can be freely obtained. Because of the short revisiting rate (1 day), the problem of cloud contamination can be reduced by using multi-date composites. With high data availability in

**Table 1**
Comparisons of the performance of models developed for individual bamboo species with and without elevation information, based on the results of 20 model runs.

| | Arrow bamboo | | Umbrella bamboo | |
|---|---|---|---|---|
| | Without elevation | With elevation | Without elevation | With elevation |
| Kappa[a] | $0.461 \pm 0.017$ | $0.681 \pm 0.015$ | $0.658 \pm 0.022$ | $0.703 \pm 0.019$ |
| *p*-value of Mann–Whitney test | $<10^{-10}$ | | $<10^{-4}$ | |
| AUC[a] | $0.798 \pm 0.009$ | $0.906 \pm 0.004$ | $0.900 \pm 0.005$ | $0.920 \pm 0.005$ |
| *p*-value of Mann–Whitney test | $<10^{-7}$ | | $<10^{-4}$ | |
| Threshold for MPA[a] | $0.211 \pm 0.015$ | $0.229 \pm 0.009$ | $0.192 \pm 0.013$ | $0.199 \pm 0.013$ |
| Proportion of MPA to study area[a] | $0.476 \pm 0.009$ | $0.223 \pm 0.005$ | $0.297 \pm 0.008$ | $0.212 \pm 0.005$ |
| *p*-value of Mann–Whitney test | $<10^{-10}$ | | $<10^{-5}$ | |

[a] Values are shown as mean $\pm 2$ SEM.

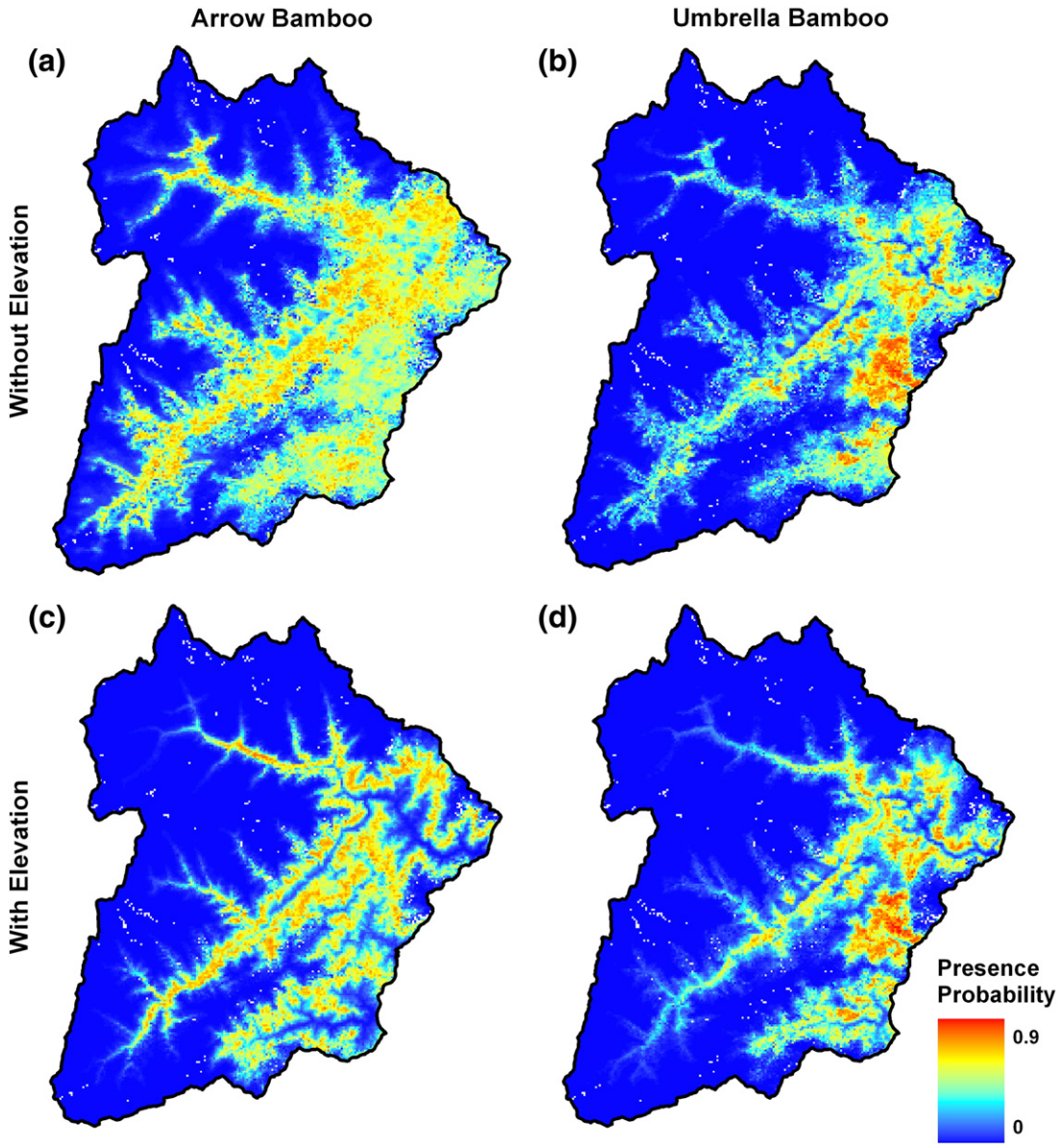


**Fig. 6.** Spatial distribution of arrow and umbrella bamboo across Wolong Nature Reserve. Mean presence probabilities of pixels were calculated over 20 runs of the individual bamboo distribution models containing only 11 phenology metrics (a and b) and the models containing the11 phenology metrics plus elevation (c and d). Pixels where phenology metrics could not be determined in at least two years between 2001 and 2003 from a smoothed curve of a time series of WDRVI values by TIMESAT are represented in white.

terms of both space and time, this approach not only can be easily applied to mapping understory vegetation across large geographic areas, but also has the potential for monitoring its temporal dynamics.

In addition, our approach may not be limited to specific understory species or specific areas and time periods because of its generality. Similar to some previous methods (Chastain & Townsend, 2007; Resasco et al., 2007; Wang et al., 2009b), our approach is also based on the phenological difference between over and understory vegetation. However, our approach uses a time series of MODIS data to capture phenological differences throughout a whole year, rather than using a single image to detect differences on a specific date. Therefore, our approach does not need prior knowledge or testing on the optimal dates on which the phenological difference between over and understory canopy components can be detected. It also does not need re-testing and adjusting the optimal dates to account for the inter-annual variability of vegetation phenology when the approach is applied to monitoring temporal dynamics (Resasco et al., 2007). In addition, as required by a GIS expert system for adjusting maps derived from remotely sensed data (Wang et al., 2009a), knowledge on the relationships between the distribution of understory vegetation and environmental variables is not necessary in our approach. Although the relationships can effectively improve the accuracy of mapping (Wang et al., 2009a), they are specific to particular vegetation types, understory species, and geographic areas. Therefore, without the requirement of specific knowledge, our approach is more general and thus is easily applicable to other vegetation types, understory species, and geographic locations.

An additional advantage of our approach is its flexibility and extensibility. Although prior knowledge on the species–environment relationships is not necessary, if available, the new approach can incorporate this information easily to extend its ability to separate different understory species. In this study, we showed that the approach with only the phenology metrics could not differentiate individual bamboo species effectively from the overall bamboo distribution because there was no significant difference in most phenology metrics between all bamboo pixels versus those with arrow or umbrella bamboo (Fig. 3). However, by incorporating elevation as an additional predictor variable,

we significantly improved the ability of our approach to separate the spatial distributions of the two species. Therefore, while our approach has its generality for detecting overall understory vegetation or groups of species with similar phenological characteristics across large areas, it can be applied to mapping individual species within specific areas by adding species- and/or area-specific information, such as elevation in this study. Contrasting to previous approaches which focused on either a group of similar species (Korpela, 2008; Linderman et al., 2004; Wang et al., 2009a) or a single species (Resasco et al., 2007; Wang et al., 2009b), our approach provides a tool to separate individual species from a group of similar ones. This advantage would be valuable for the assessment and management of understory species biodiversity.

Like any other methods, the approach developed in this study also has some limitations. First, there is always a compromise between spatial and temporal resolutions of remotely sensed data. By using WDRVI derived from MODIS data, our approach mapped understory vegetation with a spatial resolution of 250×250 m/pixel. Although this resolution is coarser than those of the previous approaches which use higher spatial resolution data, such as Landsat (e.g., Linderman et al., 2004), ASTER (e.g., Wang et al., 2009a) and LiDAR (e.g., Korpela, 2008), a previous study has shown that a time series of MODIS data performs as good as a Landsat image on mapping wildlife habitat because the finer temporal resolution of MODIS data can compensate their disadvantage of coarser spatial resolution (Viña et al., 2008). Even though this study tends to underestimate the model accuracy due to the use of presence/background, rather than presence/absence validation data, the kappa values of the overall bamboo model and the individual bamboo models with elevation generated in this study are comparable to, or even higher than, the values reported in previous studies mapping understory bamboo using higher resolution remotely sensed data (Linderman et al., 2004; Wang et al., 2009a,b). In addition, coarse spatial resolutions may be detailed enough to reveal biologically and ecologically meaningful information in studies and applications where finer spatial resolutions are not necessary, such as those used for characterizing the habitat of wildlife species with large home ranges, as the giant pandas (Schaller et al., 1985).

Second, this approach can only be applied to mapping the understory vegetation whose presence causes detectable differences in phenological characteristics. In this study, we found phenological differences between forest pixels with understory bamboo and background pixels of forests due to the high biomass and rapid growth of bamboo species. However, many understory plant species, including several non-native invasive species, have the ability to form dense understory layers and affect forest structure and function (Royo & Carson, 2006; Urgenson et al., 2009). Therefore, we believe that our approach can be applied to mapping many other understory species whose presence causes differences in land surface phenology.

Finally, calculating phenology metrics from a time series of WDRVI values derived from MODIS data requires more data processing time and computational resources than many previous methods. However, a global phenology product with a spatial resolution of 1 km (MOD12Q2, Zhang et al., 2003), and a 250 m product for North America (http://accweb.nascom.nasa.gov/), are being generated from MODIS data and being made freely accessible. In addition, the recent availability of software especially developed for extracting phenological characteristics from remotely sensed data (e.g., TIMESAT, Jönsson & Eklundh, 2004) has made the data processing easier and more efficient. With the growing interests and continuous improvements in related research on land surface phenology (Morisette et al., 2009), more data and improved tools will become available in the near future.

## 5. Conservation implications and conclusions

Understory vegetation not only has important contributions to and significant effects on the biodiversity of plant species in forest ecosystems (Gilliam, 2007; Royo & Carson, 2006), but also shapes the environments and provides resources for many wildlife species (Deal, 2007; Díaz et al., 2005; Hagar, 2007). Therefore, understanding the spatial patterns and temporal dynamics of understory vegetation is important for biodiversity conservation and habitat management. In this study, we developed an effective and practical approach for mapping understory vegetation using phenological characteristics derived from a time series of remotely sensed data. Due to the easy access, global coverage, and temporally continuous availability of MODIS data, our approach solves the problem of limited data availability that other methods may encounter when applied to larger spatial extents or finer temporal resolutions. Without the need of prior and specific information on the phenological difference between over and understory vegetation and on the relationships between understory vegetation and environmental variables, our approach can be easily applied to different species in different geographic areas. Due to its flexibility and extensibility, besides detecting general understory vegetation, the approach can be also used to differentiate individual species by incorporating species-specific information.

The approach developed in this study could provide valuable information for ecosystem management and for biodiversity conservation. For example, while remote sensing has been widely used to map and monitor the distribution of invasive plants across large spatial extents (Asner & Vitousek, 2005; Huang & Asner, 2009), its application for invasive understory species is limited (but see Asner et al., 2008; Resasco et al., 2007). Because of high biomass and rapid growth of many invasive species and their strong influence on species compositions, which may alter the land surface phenology, the approach developed in this study could provide a useful tool for the management of invasive understory plants at broad spatial scales.

In addition, wildlife habitat management and conservation could also benefit from the new approach. Understory bamboo species, for example, are staple food for giant pandas and one of the most important factors determining the quality of giant panda habitat (Bearer et al., 2008; Liu et al., 1999; Reid et al., 1989; Schaller et al., 1985). Without the essential information on bamboo distribution, a habitat evaluation may overestimate the carrying capacity of the giant panda by more than 40% (Linderman et al., 2005). Besides providing the distribution patterns of overall understory bamboo across large areas for panda habitat evaluations, our approach can also map individual species. Because different bamboo species have unequal contributions to comprising giant pandas' diet and determining habitat quality (Schaller et al., 1985), identifying the distribution of individual bamboo species may provide more detailed information for characterizing panda habitat. Furthermore, with the individual species information, the potential impacts on panda habitat of species-specific dynamics of understory bamboo (e.g., mass die-offs following flowering) can be incorporated into management planning. Since many other wildlife species around the world also depend on the understory vegetation whose information on spatio-temporal dynamics across large spatial extents is unavailable, habitat management and conservation of those species might benefit from the approach we developed in this study as well.

## Acknowledgements

This study was supported by the U.S. National Science Foundation (Dynamics of Coupled Natural and Human Systems and Partnership for International Research and Education), the National Aeronautics and Space Administration (Land Use/Land Cover Change program and Terrestrial Ecology and Biodiversity program), Michigan Agricultural Experiment Station, and the National Natural Science Foundation of China (grants 40901289 and 40321101). We thank Dr. Lars Eklundh from Lund University, Sweden for his help with using TIMESAT, and Dr. Steven Phillips from AT&T Labs Research for providing theoretical and practical help on running the Maxent software. We also thank two anonymous reviewers as well as Dr. Scott Goetz, Associate Editor, for their constructive and helpful comments and suggestions. We gratefully

acknowledge all participants in the Third National Giant Panda Survey for the field data within Wolong Nature Reserve, and the Land Processes Distributed Active Archive Center (LP DAAC), located at the U.S. Geological Survey (USGS) Earth Resources Observation and Science (EROS) Center (lpdaac.usgs.gov), for the MODIS data used in the study.

## References


Ahl, D. E., Gower, S. T., Burrows, S. N., Shabanov, N. V., Myneni, R. B., & Knyazikhin, Y. (2006). Monitoring spring canopy phenology of a deciduous broadleaf forest using MODIS. *Remote Sensing of Environment*, *104*, 88−95.

Araújo, M. B., Pearson, R. G., Thuiller, W., & Erhard, M. (2005). Validation of species–climate impact models under climate change. *Global Change Biology*, *11*, 1504−1513.

Asner, G. P., Hughes, R. F., Vitousek, P. M., Knapp, D. E., Kennedy-Bowdoin, T., Boardman, J., Martin, R. E., Eastwood, M., & Green, R. O. (2008). Invasive plants transform the three-dimensional structure of rain forests. *Proceedings of the National Academy of Sciences of the United States of America*, *105*, 4519−4523.

Asner, G. P., & Vitousek, P. M. (2005). Remote analysis of biological invasion and biogeochemical change. *Proceedings of the National Academy of Sciences of the United States of America*, *102*, 4383−4386.

Bearer, S., Linderman, M., Huang, J., An, L., He, G., & Liu, J. (2008). Effects of fuelwood collection and timber harvesting on giant panda habitat use. *Biological Conservation*, *141*, 385−393.

Chastain, R. A., Jr., & Townsend, P. A. (2007). Use of Landsat ETM and topographic data to characterize evergreen understory communities in Appalachian deciduous forests. *Photogrammetric Engineering & Remote Sensing*, *73*, 563−575.

Cohen, J. (1960). A coefficient of agreement for nominal scales. *Education and Psychological Measurement*, *20*, 37−46.

de Beurs, K. M., & Henebry, G. M. (2004). Land surface phenology, climatic variation, and institutional change: Analyzing agricultural land cover change in Kazakhstan. *Remote Sensing of Environment*, *89*, 497−509.

de Beurs, K. M., & Henebry, G. M. (2005). Land surface phenology and temperature variation in the international Geosphere–Biosphere program high-latitude transects. *Global Change Biology*, *11*, 779−790.

Deal, R. L. (2007). Management strategies to increase stand structural diversity and enhance biodiversity in coastal rainforests of Alaska. *Biological Conservation*, *137*, 520−532.

DeFries, R., Hansen, M., & Townshend, J. (1995). Global discrimination of land cover types from metrics derived from AVHRR pathfinder data. *Remote Sensing of Environment*, *54*, 209−222.

Díaz, I. A., Armesto, J. J., Reid, S., Sieving, K. E., & Willson, M. F. (2005). Linking forest structure and composition: Avian diversity in successional forests of Chiloé Island, Chile. *Biological Conservation*, *123*, 91−101.

Elith, J., Graham, C. H., Anderson, R. P., Dudik, M., Ferrier, S., Guisan, A., Hijmans, R. J., Huettmann, F., Leathwick, J. R., Lehmann, A., Li, J., Lohmann, L. G., Loiselle, B. A., Manion, G., Moritz, C., Nakamura, M., Nakazawa, Y., Overton, J. M., Peterson, A. T., Phillips, S. J., Richardson, K., Scachetti-Pereira, R., Schapire, R. E., Soberon, J., Williams, S., Wisz, M. S., & Zimmermann, N. E. (2006). Novel methods improve prediction of species' distributions from occurrence data. *Ecography*, *29*, 129−151.

Engler, R., Guisan, A., & Rechsteiner, L. (2004). An improved approach for predicting the distribution of rare and endangered species from occurrence and pseudo-absence data. *Journal of Applied Ecology*, *41*, 263−274.

Eriksson, H. M., Eklundh, L., Kuusk, A., & Nilson, T. (2006). Impact of understory vegetation on forest canopy reflectance and remotely sensed LAI estimates. *Remote Sensing of Environment*, *103*, 408−418.

Estades, C. F., & Temple, S. A. (1999). Deciduous-forest bird communities in a fragmented landscape dominated by exotic pine plantations. *Ecological Applications*, *9*, 573−585.

FAO. (1995). *Non-wood forest products for rural income and sustainable development.* Rome, Italy: Food and Agriculture Organization Non-Wood Forest Products No. 7.

Fielding, A. H., & Bell, J. F. (1997). A review of methods for the assessment of prediction errors in conservation presence/absence models. *Environmental Conservation*, *24*, 38−49.

Friedl, M., Henebry, G., Reed, B., Huete, A., White, M., Morisette, J., Nemani, R., Zhang, X., & Myneni, R. (2006). *Land surface phenology NASA white paper.* ftp://ftp.iluci.org/Land_ESDR/Phenology_Friedl_whitepaper.pdf

Gilliam, F. S. (2007). The ecological significance of the herbaceous layer in temperate forest ecosystems. *BioScience*, *57*, 845−858.

Gitelson, A. A. (2004). Wide Dynamic Range Vegetation Index for remote quantification of biophysical characteristics of vegetation. *Journal of Plant Physiology*, *161*, 165−173.

Hagar, J. C. (2007). Wildlife species associated with non-coniferous vegetation in Pacific Northwest conifer forests: A review. *Forest Ecology and Management*, *246*, 108−122.

Hanley, J. A., & Mcneil, B. J. (1982). The meaning and use of the area under a ROC curve. *Radiology*, *143*, 29−36.

Hansen, M. C., DeFries, R. S., Townshend, J. R. G., & Sohlberg, R. (2000). Global land cover classification at 1 km spatial resolution using a classification tree approach. *International Journal of Remote Sensing*, *21*, 1331−1364.

Henebry, G. M., Viña, A., & Gitelson, A. A. (2004). The Wide Dynamic Range Vegetation Index and its potential utility for gap analysis. *GAP Analysis Program Bulletin*, *12*, 50−56.

Huang, C., & Asner, G. (2009). Applications of remote sensing to alien invasive plant studies. *Sensors*, *9*, 4869−4889.

Huang, C., Geiger, E. L., Van Leeuwen, W. J. D., & Marsh, S. E. (2009). Discrimination of invaded and native species sites in a semi-desert grassland using MODIS multi-temporal data. *International Journal of Remote Sensing*, *30*, 897−917.

Iqbal, M. (1993). *International trade in non-wood forest products. An overview.* Rome, Italy: Food and Agriculture Organization.

Jensen, J. R. (2007). *Remote sensing of the environment: An earth resource perspective.* Upper Saddle River, NJ: Pearson Prentice Hall.

Jönsson, P., & Eklundh, L. (2004). TIMESAT — A program for analysing time-series of satellite sensor data. *Computers and Geosciences*, *30*, 833−845.

Jönsson, P., & Eklundh, L. (2006). *TIMESAT — A program for analyzing time-series of satellite sensor data.* Users Guide for TIMESAT 2.3.

Korpela, I. S. (2008). Mapping of understory lichens with airborne discrete-return LiDAR data. *Remote Sensing of Environment*, *112*, 3891−3897.

Landis, J. R., & Koch, G. G. (1977). The measurement of observer agreement for categorical data. *Biometrics*, *33*, 159−174.

Lefsky, M. A., Cohen, W. B., Parker, G. G., & Harding, D. J. (2002). Lidar remote sensing for ecosystem studies. *BioScience*, *52*, 19−30.

Lenney, M. P., Woodcock, C. E., Collins, J. B., & Hamdi, H. (1996). The status of agricultural lands in Egypt: The use of multitemporal NDVI features derived from Landsat TM. *Remote Sensing of Environment*, *56*, 8−20.

Linderman, M., Bearer, S., An, L., Tan, Y., Ouyang, Z., & Liu, J. (2005). The effects of understory bamboo on broad-scale estimates of giant panda habitat. *Biological Conservation*, *121*, 383−390.

Linderman, M., Liu, J., Qi, J., An, L., Ouyang, Z., Yang, J., & Tan, Y. (2004). Using artificial neural networks to map the spatial distribution of understorey bamboo from remote sensing data. *International Journal of Remote Sensing*, *25*, 1685−1700.

Liu, C., Berry, P. M., Dawson, T. P., & Pearson, R. G. (2005). Selecting thresholds of occurrence in the prediction of species distributions. *Ecography*, *28*, 385−393.

Liu, J., Ouyang, Z., Taylor, W. W., Groop, R., Tan, Y., & Zhang, H. (1999). A framework for evaluating the effects of human factors on wildlife habitat: The case of giant pandas. *Conservation Biology*, *13*, 1360−1370.

Lloyd, D. (1990). A phenological classification of terrestrial vegetation cover using shortwave vegetation index imagery. *International Journal of Remote Sensing*, *11*, 2269−2279.

McPherson, J. M., Jetz, W., & Rogers, D. J. (2004). The effects of species' range sizes on the accuracy of distribution models: Ecological phenomenon or statistical artefact? *Journal of Applied Ecology*, *41*, 811−823.

Morisette, J. T., Jarnevich, C. S., Ullah, A., Cai, W., Pedelty, J. A., Gentle, J. E., Stohlgren, T. J., & Schnase, J. L. (2006). A tamarisk habitat suitability map for the continental United States. *Frontiers in Ecology and the Environment*, *4*, 11−17.

Morisette, J. T., Richardson, A. D., Knapp, A. K., Fisher, J. I., Graham, E. A., Abatzoglou, J., Wilson, B. E., Breshears, D. D., Henebry, G. M., Hanes, J. M., & Liang, L. (2009). Tracking the rhythm of the seasons in the face of global change: Phenological research in the 21st century. *Frontiers in Ecology and the Environment*, *7*, 253−260.

Nilsson, M. -C., & Wardle, D. A. (2005). Understory vegetation as a forest ecosystem driver: Evidence from the northern Swedish boreal forest. *Frontiers in Ecology and the Environment*, *3*, 421−428.

Pearce, J., & Ferrier, S. (2000). Evaluating the predictive performance of habitat models developed using logistic regression. *Ecological Modelling*, *133*, 225−245.

Peckham, S. D., Ahl, D. E., & Gower, S. T. (2009). Bryophyte cover estimation in a boreal black spruce forest using airborne lidar and multispectral sensors. *Remote Sensing of Environment*, *113*, 1127−1132.

Phillips, S. J., Anderson, R. P., & Schapire, R. E. (2006). Maximum entropy modeling of species geographic distributions. *Ecological Modelling*, *190*, 231−259.

Phillips, S. J., & Dudík, M. (2008). Modeling of species distributions with Maxent: New extensions and a comprehensive evaluation. *Ecography*, *31*, 161−175.

Qin, Z., Taylor, A., & Cai, X. (1993). *Dynamic succession of the bamboo and forests in panda habitat in Wolong.* Beijing: China Forestry Publishing House.

Rautiainen, M., Suomalainen, J., Mottus, M., Stenberg, P., Voipio, P., Peltoniemi, J., & Manninen, T. (2007). Coupling forest canopy and understory reflectance in the Arctic latitudes of Finland. *Remote Sensing of Environment*, *110*, 332−343.

Reed, B. C., Brown, J. F., VanderZee, D., Loveland, T. R., Merchant, J. W., & Ohlen, D. O. (1994). Measuring phenological variability from satellite imagery. *Journal of Vegetation Science*, *5*, 703−714.

Reid, D. G., Hu, J., Dong, S., Wang, W., & Huang, Y. (1989). Giant panda *Ailuropoda melanoleuca* behaviour and carrying capacity following a bamboo die-off. *Biological Conservation*, *49*, 85−104.

Reid, D. G., Taylor, A. H., Hu, J., & Qin, Z. (1991). Environmental influences on bamboo *Bashania fangiana* growth and implications for giant panda conservation. *Journal of Applied Ecology*, *28*, 855−868.

Resasco, J., Hale, A. N., Henry, M. C., & Gorchov, D. L. (2007). Detecting an invasive shrub in a deciduous forest understory using late-fall Landsat sensor imagery. *International Journal of Remote Sensing*, *28*, 3739−3745.

Roughgarden, J., Running, S. W., & Matson, P. A. (1991). What does remote sensing do for ecology? *Ecology*, *72*, 1918−1922.

Royo, A. A., & Carson, W. P. (2006). On the formation of dense understory layers in forests worldwide: Consequences and implications for forest dynamics, biodiversity, and succession. *Canadian Journal of Forest Research*, *36*, 1345−1362.

Schaller, G. B., Hu, J., Pan, W., & Zhu, J. (1985). *The giant pandas of Wolong.* Chicago, Illinois: University of Chicago Press.

Schwartz, M. D., & Reed, B. C. (1999). Surface phenology and satellite sensor-derived onset of greenness: An initial comparison. *International Journal of Remote Sensing*, *20*, 3451−3457.

Sheskin, D. (2000). *Handbook of parametric and nonparametric statistical procedures.* Boca Raton: Chapman & Hall/CRC.

State Forestry Administration (2006). *The third national survey report on giant panda in China.* Beijing: Science Press.

Swets, J. A. (1988). Measuring the accuracy of diagnostic systems. *Science*, *240*, 1285−1293.

Taylor, A. H., Huang, J. Y., & Zhou, S. Q. (2004). Canopy tree development and undergrowth bamboo dynamics in old-growth *Abies-Betula* forests in Southwestern China: A 12-year study. *Forest Ecology and Management*, *200*, 347−360.

Taylor, A. H., Jang, S. W., Zhao, L. J., Liang, C. P., Miao, C. J., & Huang, J. Y. (2006). Regeneration patterns and tree species coexistence in old-growth *Abies-Picea* forests in southwestern China. *Forest Ecology and Management*, *223*, 303−317.

Taylor, A. H., & Qin, Z. (1993). Structure and dynamics of bamboos in the Wolong Natural Reserve, China. *American Journal of Botany*, *80*, 375−384.

Townsend, P., & Walsh, S. (2001). Remote sensing of forested wetlands: Application of multitemporal and multispectral satellite imagery to determine plant community composition and structure in southeastern USA. *Plant Ecology*, *157*, 129−149.

Urgenson, L. S., Reichard, S. H., & Halpern, C. B. (2009). Community and ecosystem consequences of giant knotweed (*Polygonum sachalinense*) invasion into riparian forests of western Washington, USA. *Biological Conservation*, *142*, 1536−1541.

Vierling, K. T., Vierling, L. A., Gould, W. A., Martinuzzi, S., & Clawges, R. M. (2008). Lidar: Shedding new light on habitat characterization and modeling. *Frontiers in Ecology and the Environment*, *6*, 90−98.

Viña, A., Bearer, S., Chen, X., He, G., Linderman, M., An, L., Zhang, H., Ouyang, Z., & Liu, J. (2007). Temporal changes in giant panda habitat connectivity across boundaries of Wolong Nature Reserve, China. *Ecological Applications*, *17*, 1019−1030.

Viña, A., Bearer, S., Zhang, H., Ouyang, Z., & Liu, J. (2008). Evaluating MODIS data for mapping wildlife habitat distribution. *Remote Sensing of Environment*, *112*, 2160−2169.

Viña, A., Gitelson, A. A., Rundquist, D. C., Keydan, G., Leavitt, B., & Schepers, J. (2004). Monitoring maize (*Zea mays* L.) phenology with remote sensing. *Agronomy Journal*, *96*, 1139−1147.

Viña, A., Henebry, G. M., & Gitelson, A. A. (2004). Satellite monitoring of vegetation dynamics: Sensitivity enhancement by the Wide Dynamic Range Vegetation Index. *Geophysical Research Letters*, *31*, L04503.

Wang, T. J., Skidmore, A. K., & Toxopeus, A. G. (2009). Improved understorey bamboo cover mapping using a novel hybrid neural network and expert system. *International Journal of Remote Sensing*, *30*, 965−981.

Wang, T. J., Skidmore, A. K., Toxopeus, A. G., & Liu, X. (2009). Understory bamboo discrimination using a winter image. *Photogrammetric Engineering & Remote Sensing*, *75*, 37−47.

Wolong Nature Reserve and Sichuan Normal College (Ed.) (1992). *The animal and plant resources and protection of Wolong Nature Reserve*. Chengdu: Sichuan Publishing House of Science & Technology.

Zhang, X., Friedl, M. A., Schaaf, C. B., Strahler, A. H., Hodges, J. C. F., Gao, F., Reed, B. C., & Huete, A. (2003). Monitoring vegetation phenology using MODIS. *Remote Sensing of Environment*, *84*, 471−475.

Zweig, M., & Campbell, G. (1993). Receiver-operating characteristic (ROC) plots: A fundamental evaluation tool in clinical medicine [published erratum appears in Clin Chem 1993 Aug;39(8):1589]. *Clinical Chemistry*, *39*, 561−577.